

Self-organized quantum transitions in a spin-electron coupled system

W. Koshibae¹, N. Furukawa^{2,3}, and N. Nagaosa^{1,4}

¹*Cross-Correlated Materials Research Group (CMRG), RIKEN, Saitama 351-0198, Japan*

²*Aoyama-Gakuin University, 5-10-1, Fuchinobe, Sagami-hara, Kanagawa 229-8558, Japan*

³*ERATO-Multiferroics, JST, c/o Department of Applied Physics,
The University of Tokyo, Tokyo 113-8656, Japan*

⁴*Department of Applied Physics, The University of Tokyo, Tokyo 113-8656, Japan*

We investigate quantum dynamics of the excited electronic states in the double-exchange model at half-filling by solving coupled equations for the quantum evolution of electrons and Landau-Lifshits-Gilbert equation for classical spins. The non-adiabatic quantum transitions driving the relaxation are coordinated through the self-organized space-time structure of the electron/spin dynamics leading to a resonant precession analogous to the ESR process.

In the strongly correlated electron systems such as the transition metal oxides, the rich phases including the spin/charge/orbital ordered states and superconducting state are realized by the electron-electron and electron-lattice interactions [1]. An essential feature of the strongly correlated electron systems is the appearance of the internal degrees of freedom such as spins. The dynamics of the electrons with the strong interaction can be translated to the motion of the electrons in the background of the fluctuating *spin fields* via the Stratonovich-Hubbard transformation [1]. Therefore, the quantum dynamics of the correlated electrons can be formulated as that of the coupled dynamics of the spins and electrons.

In particular, the time-dependent quantum dynamics in nonequilibrium states are now an issue of intensive interests. An example is the photo-induced quantum dynamics of the spin-electron coupled systems [2, 3, 4, 5, 6]. In the systems, the dynamics of the spins plays a crucial role in the relaxation of the electrons after the photo-excitations leading to distinct features compared with the usual semiconductors or band insulators, where the electron-phonon interaction plays the major role in the relaxation. For example, the photo-induced ferromagnetism can lead to the metallic state in manganites due to enhanced kinetic energy in the double exchange interaction [5, 6] in sharp contrast to the self-trapping of the small polaron in the band insulators. This means that the coupled dynamics of the spins and electrons must be treated as the many-body collective phenomena in the correlated electron systems. The nonequilibrium quantum phenomena still remain challenges for theoretical study [7, 8, 9]. In general, it is not easy to capture the nature of the many-body electronic state, and our study below is complementary to the previous works giving a semiclassical picture for quantum dynamics for larger size/higher dimensional systems.

In this paper, we study the relaxation dynamics of the excited states in the double-exchange model [10], where the classical spins are coupled to the conduction electrons. This model has the advantage that the fully quantum dynamics of the electrons combined with the classical motion of spins can be simulated, providing a clear physical picture. This way of describing the correlation effect is essentially justified for the magnetically ordered state where the (staggered) magnetization behaves as semi-classical object. We found that the self-organized

space-time structure of the spins and electrons is formed through the *quantum* transition as shown below.

We start with the Hamiltonian on the square lattice,

$$\hat{H} = -t \sum_{\langle ij \rangle, s} c_{is}^\dagger c_{js} + h.c. - J_H \sum_{iss'} c_{is}^\dagger c_{is'} \vec{\sigma}_{ss'} \cdot \vec{S}_i, \quad (1)$$

where $\langle ij \rangle$ denotes a nearest-neighbor pair, s and s' are indices for electron spin, respectively, and $\vec{\sigma}_{ss'}$ is given by Pauli matrices. The local spins, \vec{S}_i 's, are taken to be classical vectors with magnitude S . Other notations are standard. We consider the half-filled case, i.e., one electron per site.

Using finite size systems, we numerically investigate the time evolution of the electronic states and local spins. The equation of motion for the local spins is expressed by the Landau-Lifshitz-Gilbert (LLG) equation, $\dot{\vec{S}}_i = -J_H \langle \vec{\sigma}_i \rangle \times \vec{S}_i + \alpha \vec{S}_i \times \dot{\vec{S}}_i$, where $\langle \vec{\sigma}_i \rangle$ is the expectation value of electron spin at site i , and the Gilbert damping constant $S\alpha$ describes all the other relaxation processes of the spins than the coupling to the conduction electrons. When $\langle \vec{\sigma}_i \rangle$ is fixed, the solution of the LLG equation is given by $\phi_i(T) = -[(SJ_H/t)\langle \vec{\sigma}_i \rangle / (1 + (S\alpha)^2)](t/S)T$, and $\theta_i(T) = 2 \tan^{-1}[\tan(\theta_{i0}/2) \exp(S\alpha\phi_i)]$, where (θ_i, ϕ_i) is the polar and azimuthal angles of \vec{S}_i in the local spin coordinate where z axis is parallel to $\langle \vec{\sigma}_i \rangle$ and initial value of ϕ_i is zero, and T is time. The initial value of θ_i is written by θ_{i0} . Evolution of the electronic state $|\Phi(T)\rangle$ is given by $|\Phi(T)\rangle = \hat{U}(T)|\Phi(0)\rangle$, where $\hat{U}(T)$ is a unitary operator for the time evolution. If $\{\vec{S}_i\}$ are fixed, we have $\hat{U}(T) = \exp(-i\hat{H}T)$. We successively calculate the evolution of the electronic state and the LLG equation for a small time increment ΔT to investigate evolutions of the system in total. The changes in $\{\vec{S}_i\}$ and $|\Phi(T)\rangle$ are reflected to the calculation through \hat{H} and $\{\langle \vec{\sigma}_i \rangle\}$.

The Hamiltonian (1) is expressed by a bilinear form of fermion operators. In such a case, it is known that the electronic state $|\Phi(T)\rangle$ remains to be a single Slater determinant state if the initial state is so [11]. This allows us to increase the system size, which is advantageous for investigation of low-frequency dynamics with accuracies.

Figure 1 shows the calculated result on the system of size 8×8 with the periodic boundary condition. As a typical example, a parameter set, $t=1$, $SJ_H=2$, $S\alpha=1$, $S=1$, $\Delta T=0.008$, is used. The lower panel of Fig. 1(a)

is the time (T) dependence of the energy level structure. The Fermi level is taken to be zero. At around $T \sim 0$, we clearly see the energy gap $2SJ_H$ between upper and lower energy bands in the lower panel of Fig. 1(a). We prepare the initial state in the following way: The ground state of the double-exchange model (1) at half filling is the antiferromagnetic (AF) insulating state because of the perfect nesting-condition in this system. In order to mimic the thermal fluctuation, we introduce a random tilting of each spin from the AF configuration up to 0.1 radian which corresponds to the state with an excitation energy of $\sim 0.001t$ from the ground state. The energy band is divided into upper and lower ones. For the initial state, we fill up the lower energy band, and then transfer two electrons from the lowest eigenstates in the lower energy band to the two highest levels in the upper energy band. In the upper panel of Fig. 1(a), the number of electron of the *highest* (*lowest*) energy states in the upper energy band is shown by the broken (dotted) line, and the solid line is the number of electron in the upper energy band. Figures 1(b)-(e) show the time dependence of the configuration of the local spins, while Figs. 1(f)-(i) are the corresponding local energy density defined by the expectation value of $-(t/2) \sum_{\rho,s} (c_{is}^\dagger c_{\rho s} + h.c.) - J_H \sum_{ss'} c_{is}^\dagger c_{is'} \vec{\sigma}_{ss'} \cdot \vec{S}_i$, where ρ runs over the nearest-neighbor sites of i . In the Figs. 1(f)-(i), the energy of the ground state is taken to be zero.

In the numerical simulation, we find several distinct time regions, Stage (I)-(IV):

Stage (I): Precursor process. Up to $T \sim 20$, there occurs almost no change and the spins are almost frozen at the initial configuration. Figure 1(f) shows the energy density at $T=8$, showing that the excitation energy is almost uniformly distributed due to the extended nature of the excited states. However, small deviation from the AF configuration grows eventually leading to the next stage.

Stage (II): Self-organization process. At this stage, the system shows spatial inhomogeneity with energy dissipation. At around $T=20 \sim 40$, the spins start to move, and the electrons at the highest 2 energy states start to spread into lower energy states within the upper energy band (see the broken line in the upper panel of Fig. 1(a)). Up to $T \sim 170$, the deviation of the spins are not so large moving around the original direction as shown by the snapshot in Fig. 1(c) at $T=80$. This small amplitude spin fluctuation can induce the intra-band transitions of the excited electrons to lower and lower energy state. It is noted that the total energy decreases due to an energy dissipation originate from the Gilbert damping. The energy distribution shows the gentle spatial dependence with the reduced average as shown in Fig. 1(g) for $T=80$. This means that the electronic wavefunctions are rather extended though slightly disturbed by the small tilting of the spins.

Stage (III): Relaxation process with interband transition. The inhomogeneity developed in the previous stage brings about a remarkable localization behavior and derives a dynamic relaxation process with the interband transition. At around $T \sim 220$, the electronic and local-spin structures show a dramatic change characterized by the large amplitude motion of a local spin marked by an

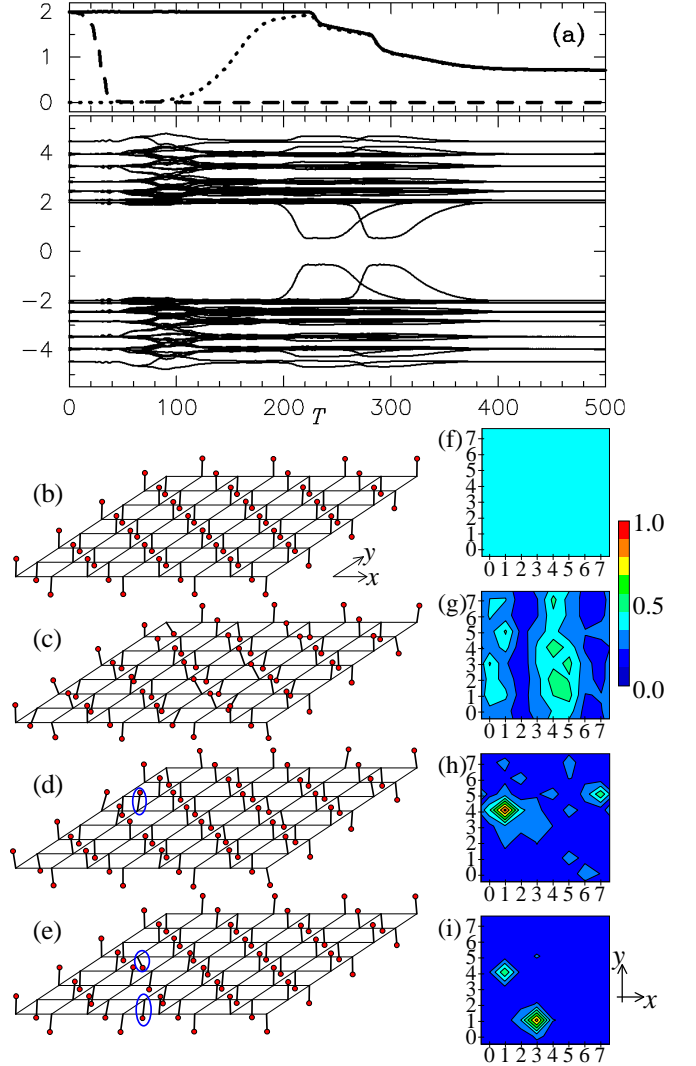


FIG. 1: (Color online) Time evolution of the double exchange model (see text). (a) The lower panel shows the time (T) dependence of the energy level structure. In the upper panel, the number of electrons in the upper energy band (solid line), in the *highest* two energy states (broken line), and in the *lowest* energy states of the upper energy band (dotted line) are shown. Configuration of local spins at $T=8, 80, 224$, and 288 are presented in (b), (c), (d) and (e), respectively. Dot indicates the head of local spin. The local spins marked by ellipses in (d) and (e) are strongly deviated from the ground state. Figures (f), (g), (h) and (i) show the distribution of excitation energy density measured from the ground state at $T=8, 80, 224$, and 288 , respectively.

ellipse in Fig. 1(d). This motion starts at $T \sim 200$. At this time, the excited electrons reach the *lowest* states in the upper energy band as shown by the dotted line in the upper panel of Fig. 1(a), and find the localized place to relax furthermore. That is, the localization of the electronic state together with the large-amplitude local-spin motion with the polar angle of the order of π occurs concomitantly. This corresponds to a pair of the in-gap energy levels split off from the edge of the upper and lower energy bands at around $T \approx 200$, as seen in the lower panel of Fig. 1(a). When the separation of in-gap energy levels is smallest, the number of excited electrons decreases rapidly. After that, the local spin re-

covers toward its original direction, and the in-gap states merges again into the upper and lower energy bands. As shown in Fig. 1(h) for $T=224$, the excitation energy is concentrated around this local spin, which in turn drives a motion of that local spin. In the same way, the relaxation dynamics with interband transition occurs again at $T\sim 300$, around another site (see Figs. 1(a), (e) and (i)). This transition through the in-gap states reminds us the Landau-Zener mechanism. However, a more thorough study given below reveals that it is a *resonant* transition and is completely different from the Landau-Zener process.

Stage (IV): Relaxation process to a meta-stable state. After $T\sim 400$, the active motion of the local spins is finished and the alignment becomes nearly perfect AF. The excited electrons, however, remains more than ~ 0.7 in the upper energy band. This meta-stable state continues for a long time within our simulation (at least up to $T\sim 8000$).

Now we consider the quantum dynamics in more depth. As discussed below, there are two components of the local spins, i.e., the *rapid* oscillation and the *slow* motion as expressed by $\vec{S}_i = \vec{S}_i^{slow} + \vec{S}_i^{rapid}$. Let us first consider the *rapid* oscillation. Figure 2(a) shows the y -component of the local spin moving with a largest deviation from the AF ground state configuration through Stage (I) and the early period of Stage (II), and the inset is the trajectory of the local spin on the $S_x - S_y$ plane. As seen in Fig. 2(a), the local spin shows an oscillation with a period of $T_p \cong 12$, i.e., the frequency $\omega (=2\pi/T_p) \cong 0.5$. We find that this frequency ω corresponds to the difference of the energy between the highest (ε_1) and second highest (ε_2) energy levels in the lower panel of Fig. 1(a). The rapid oscillation \vec{S}_i^{rapid} is driven by time dependence of $\vec{\sigma}$ in the LLG equation: When the wavefunction has the form $|\psi(t)\rangle = c_1(t)|1\rangle + c_2(t)|2\rangle$ with $c_a(t) = c_a(0)e^{-i\varepsilon_a t}$, $\langle \vec{\sigma}_i(t) \rangle$ has the component proportional to $c_1(t)^* c_2(t) \langle 1|\vec{\sigma}_i|2 \rangle \propto e^{i(\varepsilon_1 - \varepsilon_2)t}$ and its complex conjugate. Putting this into the LLG equation, we obtain $\vec{S}_i^{rapid}(t) \propto c_1(t)^* c_2(t) \langle 1|\vec{\sigma}_i|2 \rangle \times \vec{S}_i^{slow} + h.c..$ This interpretation is consistent with the Fourier spectral weight [12] of the spin motion in Fig. 2(e), where the peak is observed around the frequency $\omega \cong 0.5$, which corresponds to $\varepsilon_1 - \varepsilon_2$ in Stage (I). This *rapid* oscillation in turn induces the transition between the state $|1\rangle$ and $|2\rangle$, analogously to the electron spin resonance (ESR) where the oscillating transverse magnetic field induces the Rabi oscillation. Figure 2(b) is the time dependence of the electron occupation number at the highest energy states at Stage (I)-(II), and it clearly shows this Rabi oscillation with the frequency (Ω) determined by the oscillation amplitude (δS^{rapid}) of \vec{S}_i^{rapid} . From Fig. 2(a), we can read the oscillation amplitude $\delta S^{rapid} \cong 0.3$, so that the frequency Ω is estimated to be $J_H \delta S^{rapid} \cong 0.6$. Therefore, the occupation number will show an oscillation with a period of $2\pi/(\Omega) \cong 5.2$. This oscillation is actually observed as shown in Fig. 2(b). With the Gilbert damping, this oscillation is the damped one and the occupation number of the lower energy state increases.

It is important to note that the spatial inhomogeneity essentially occurs with the relaxation dynamics discussed

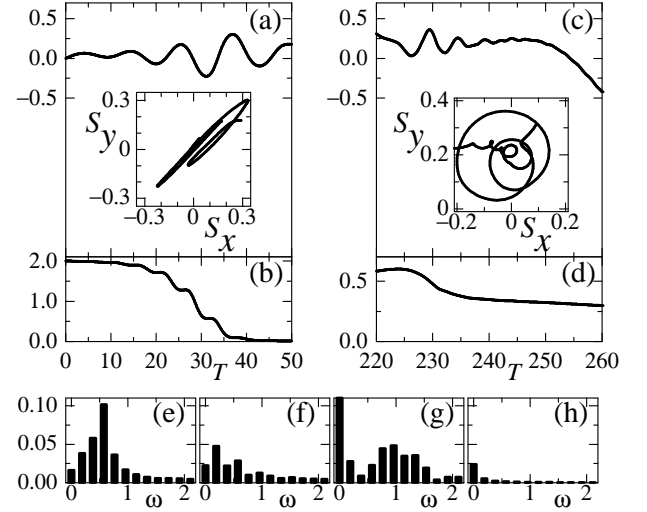


FIG. 2: Relaxation driven by *rapid* oscillation. (a) The y -component of the local spin which shows the largest deviation from the AF ground state configuration in Stage (I) and (II). The inset is the trajectory of the local spin on the $S_x - S_y$ plane. (b) The electron occupation number at the highest energy states. (c) The same with (a) but in Stage (III). (d) The electron occupation number at the lowest energy state (in-gap state) in the upper energy band. (e) The Fourier spectral weight of (a). (f) The same with (e) but $T=132$ in Stage (II). (g) The Fourier spectral weight of (c). (h) The same with (f) but $T=600$ in Stage (IV).

above. At Stage (I), the local spin alignment is almost perfect AF. In this state, the momentum is a good quantum number and the eigenvalue and eigenstate are well defined by it. With the time evolution, the excited electrons are distributed into lower energy levels, so that the spatial inhomogeneity appears as observed in the spatial distribution of the local energy density [14]. Reflecting the inhomogeneity, the magnitude of the *rapid* oscillation of the local spin depends on the sites in real space strongly. When we look at the local spins at other sites, this *rapid* oscillation is almost missing and only the slow and small amplitude motion is observed. This means that the site-selective lock-in of the *rapid* oscillation of the spins occurs self-consistently with the electronic levels before and after the transitions. This self-organized space-time structure is the most basic mechanism of the quantum transitions in the spin-electron coupled systems.

With further time evolution in Stage (II), the energy level structure becomes disordered reflecting the disordered spin configuration, and the spectral density does not show characteristic frequency in this case (see Fig. 2(f)) since it is given by many components corresponding to various $\varepsilon_n - \varepsilon_m$.

Figure 2(c) shows the motion of the local spin marked by an ellipse in Fig. 1(d) for Stage (III). As seen in the inset of Fig. 2(c), the local spin shows a *rapid* precession. Figure 2(d) shows the electron occupation number at the lowest energy state (in-gap state) in the upper energy band. In this case, however, the Rabi-oscillation behavior has not been observed. This is because the excited electrons in the states forming the bottom of the upper energy band show a cascade relaxation process, and the several frequencies are involved in those (see Fig. 2(g)). It

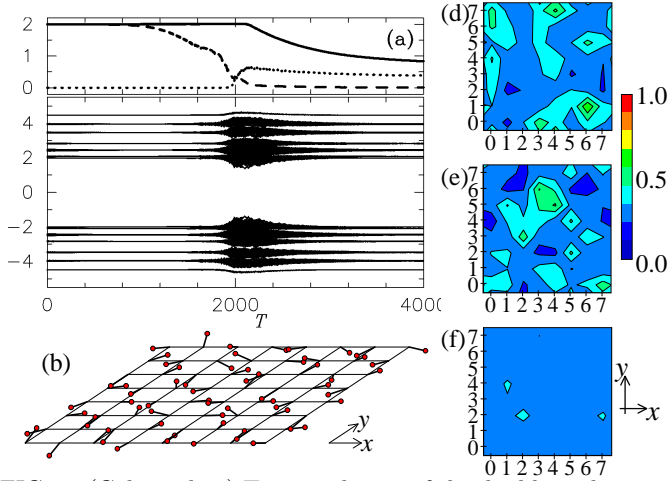


FIG. 3: (Color online) Time evolution of the double exchange model. The parameter set, $t=1$, $SJ_H=2$, $S\alpha=0.01$, $S=1$, $\Delta T=0.008$, is used. (a) The same with Fig. 1(a). (b) Structure of local spins at $T=2000$. Distribution of energy density at (d) $T=2000$, (e) $T=2100$, and (f) $T=2200$.

is seen, in fact, that at the early period of Stage (III), the excited electrons occupy the lowest energy states of the upper energy band, and from those states an in-gap state appears (see Fig. 1). Corresponding to the differences between those energy levels, the spectral density in Fig. 2(g) has the peak around $\omega \cong 1$. In other words, the inter-band transition occurs successively through those energy levels. Therefore, the dynamics similar to the ESR process is also essential for the inter-band transition in this Stage (III). In Stage (IV), there occurs no quantum transition any more because $\langle 1|\vec{\sigma}_i|2\rangle \times \vec{S}_i^{slow} = \vec{0}$ for the AF state.

Let us consider the time scale for the *slow* motion of the local spins. The deviation of the electron spin from the ground state of the excited electronic state gives a force to the local spins through the LLG equation. Therefore, $\{(1/N_{\text{eff}})J_H S\alpha/[1 + (S\alpha)^2]\}^{-1}$ determines the time scale for the motion of the local spins, where N_{eff} is the number of the sites in the real space over which the wave-

function of the excitation has the finite weight (see the solution of the LLG equation). For the plane wave states at Stage (I) and (II), $N_{\text{eff}} = N$ (the total number of the sites) and decreases as the wavefunction becomes more localized with the time evolution as seen in Figs. 1(f)-(i). In the present case, $S\alpha = 1$, a time scale of the *slow* dynamics being of the order of 100 is derived [13]. We have also studied the more realistic case of $S\alpha=0.01$ (Fig. 3). The mechanism of the relaxation dynamics for $S\alpha=0.01$ is essentially the same with the previous case. The observed time scale of the *slow* dynamics in Fig. 3(a) is about 10 times as large as that of Fig. 1(a), whereas the above simple consideration on the time scale gives about 50 times longer one compared with the case that $S\alpha = 1$. In the case for small $S\alpha$, because the *friction* is small, a large number of local spins show very active dynamics (see Fig. 3(b)). This results that the considerable spatial area (but *not* the whole area of the system) and many in-gap states are responsible for the relaxation dynamics in Stage (III) (see Figs. 3(a), (d) and (e)), whereas the strongly localized in the real space and a few in-gap states are available for the relaxation dynamics in the case that $S\alpha = 1$ (see Figs. 1(a), (h) and (i)). As a result, the relaxation process is accelerated, and the 10 times difference in the *slow* time scale appears although a hundred times difference in the magnitude of $S\alpha$ is in this case.

In summary, we have studied the relaxation dynamics of the excited state of the electron-spin coupled systems. The self-organized space-time structure of the spins and electronic state triggers the quantum transitions, and the adiabatic approximation does not work here.

The authors are grateful to Y. Tokura, M. Kawasaki, H. Matsueda, T. Tohyama, S. Ishihara, and K. Tsutsui for useful discussions. This work is supported by Grant-in-Aid for Scientific Research (Grant No. 19048015, 19048008, 17105002, 21244053, 18560043, 19014017, and 21360043) and a High-Tech Research Center project for private universities from the Ministry of Education, Culture, Sports, Science and Technology of Japan, Next Generation Supercomputing Project of Nanoscience Program, JST-CREST and NEDO.

-
- [1] M.Imada, A. Fujimori, and Y. Tokura, Rev. Mod. Phys. **70**, 1039 (1998).
 - [2] Y. Ogawa, S. Koshihara, K. Koshino, T. Ogawa, C. Urano, and H. Takagi, Phys. Rev. Lett. **84**, 3181 (2000).
 - [3] Y. Mitsumori, A. Oiwa, T. Shupinski, H. Maruki, Y. Kashimura, F. Minami, and H. MuneKata, Phys. Rev. B **69**, 033203 (2004).
 - [4] S. Koshihara, A. Oiwa, M. Hirasawa, S. Katsumoto, Y. Iye, C. Urano, and H. Takagi, and H. MuneKata, Phys. Rev. Lett. **78**, 4617 (1997).
 - [5] K. Miyano, T. Tanaka, Y. Tomioka, and Y. Tokura, Phys. Rev. Lett. **78**, 4257 (1997).
 - [6] M. Fiebig, K. Miyano, Y. Tomioka, and Y. Tokura, Science **280**, 1925 (1998).
 - [7] H. Matsueda and S. Ishihara, J. Phys. Soc. Jpn. **76**, 083703 (2007).
 - [8] H. Matsueda, A. Ando, T. Tohyama, and S. Maekawa, Phys. Rev. B **77**, 193112 (2008).
 - [9] K. Yonemitsu and N. Maeshima, Phys. Rev. B **79**, 125118 (2009).
 - [10] P.-G. de Gennes, Phys. Rev. **118**, 141 (1960).
 - [11] M. Imada and Y. Hatsugai, J. Phys. Soc. Jpn. **58**, 3752 (1989).
 - [12] For the Fourier analysis, 2^{12} points with a small time increment $\Delta T=0.008$ in units of $1/t$ are used.
 - [13] We have examined how long it takes to begin the inter-band transition in Stage (III) using 6x6, 8x8, 10x10 and 12x12 systems. In the initial state, two electrons are excited from the lowest to highest energy levels. We have confirmed that the period leading up to the inter-band transition increases linearly as a function of the system size.
 - [14] The inhomogeneity has also been observed in the spatial distribution of the magnitude of electron spins $\langle |\vec{\sigma}_i| \rangle$.